



## Electrochemical reduction of indigo in fixed and fluidized beds of graphite granules<sup>☆</sup>

A. ROESSLER, D. CRETENAND, O. DOSSENBACH\* and P. RYS

*Institute for Chemical and Bioengineering, Swiss Federal Institute of Technology (ETH), CH-8093 Zurich, Switzerland*

*(\*author for correspondence, fax: +41 1 532 1074, e-mail: dossenbach@tech.chem.ethz.ch)*

Received 27 November 2002; accepted in revised form 26 February 2003

*Key words:* anthraquinone, electrochemical reduction, fixed bed, graphite, indigo, modified electrode, quinone, vat dyes

### Abstract

Reducing agents required in the dyeing process for vat and sulfur dyes cannot be recycled and lead to problematic waste products. The electrochemical reduction of indigo on a fixed bed cathode consisting of graphite granules has been investigated by spectrophotometric experiments in laboratory cells. Experiments yield information about the kinetics and show the possibility of this process for production of water soluble leuco indigo, which offers environmental benefits. The influence of noble metals deposited on the granules and of different pretreatment methods of the graphite is demonstrated. In addition, the immobilization of quinoid molecules on the graphite surface has been investigated.

### 1. Introduction

Dyestuffs such as sulfur and vat dyes, especially indigo, play an important role in today's dyeing industry (market about 120 000 t a<sup>-1</sup>). This water insoluble dye category is applied to the fiber in the reduced soluble form (leuco dye), and, after penetration into the fibre, is converted back to the original pigment form by oxidation (Scheme 1). The disposal of dye baths and rinsing water is causing various problems, because of the surplus of reducing agents and the follow-up products from their use. Therefore, many attempts are being made to replace the environmentally unfavourable sodium dithionite as reducing agent by ecologically more attractive alternatives [1–9].

Direct electrochemical reduction of indigo would be an elegant way, because it minimizes the consumption of chemicals. Unfortunately, it is impossible at present to reduce indigo to an aqueous suspension on a planar electrode. However, it is possible to reduce solid indigo microcrystals immobilized on the surface of several electrode materials in buffered solution, and the results are very similar to those obtained for indigo dissolved in solvents [10, 11]. Thus, the limiting factor seems to be the poor contact between indigo particles and the electrode, and it is desirable to develop a reduction process by using a different reactor design based on the

intensification of the contact between the dye particles and the electrode. Recently, the precoat-layer-cell has been presented as a solution [6, 7]. Unfortunately, during the process a large pressure drop is built up over the filtration layer and there is a persistent danger of blocking the reactor.

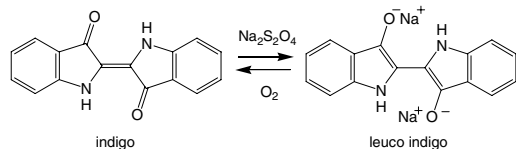
We have investigated the industrial feasibility of indigo reduction in fixed and fluidized beds of graphite granules. Graphite is a very cheap and stable material and the pressure drop over the granular material proved to be feasible. To optimize the operating conditions a great deal of work has been focused on the acceleration of the process by modification of the graphite surface by different pretreatment methods as well as the modification of the electrode surface with quinones and anthraquinones. In addition, the influence of noble metals supported on the granules has been studied.

### 2. Experimental details

#### 2.1. Chemicals

All commercially available chemicals were used as received from Fluka. Indigo was supplied from BASF, Ludwigshafen, Germany. 5-Amino-acenaphthenequinone was synthesized from acenaphthenequinone by nitration [12] and a subsequent reduction with hydrazine hydrate in the presence of an iron oxide hydroxide

<sup>☆</sup> This paper was originally presented at the 6<sup>th</sup> European Symposium on Electrochemical Engineering, Düsseldorf, Germany, September 2002.



Scheme 1. Vattling of indigo.

according to a reported general procedure [13]. All aqueous solutions were prepared with deionized water.

## 2.2. Cells

A conventional laboratory flow-through H-cell was used in preliminary experiments designed to determine whether the crucial contact between indigo particles and the electrode could be achieved. The results obtained after an optimization were then used as a guide in designing and operating a continuous larger scale flow cell to show the industrial feasibility at higher indigo concentrations.

### 2.2.1. Small scale apparatus

A small flow channel with a packed or fluidized bed was used for the experiments. The working electrode consisted of a bed of 40 g of graphite granules ( $d = 2-3$  mm). A stainless steel wire ( $d = 1.5$  mm) was located in the centre of the bed as current feeder. Ru/Ta was used as anode material, and the cell was divided into two compartments by a Nafion<sup>®</sup>-324 membrane (DuPont). The set-up of this pilot plant is given in Figure 1. The flow circuit is described in detail elsewhere [5, 8]. Current supply was from a potentiostat (Radiometer Copenhagen DEA 332, Electrochemical Interface IMT102 and Software Voltmaster2).

### 2.2.2. Large scale apparatus

As shown in Figure 2 the cell had a cylindrical concentric arrangement with central position of the counter electrode (Pt/Ru), outer position of the feeder (100 mesh

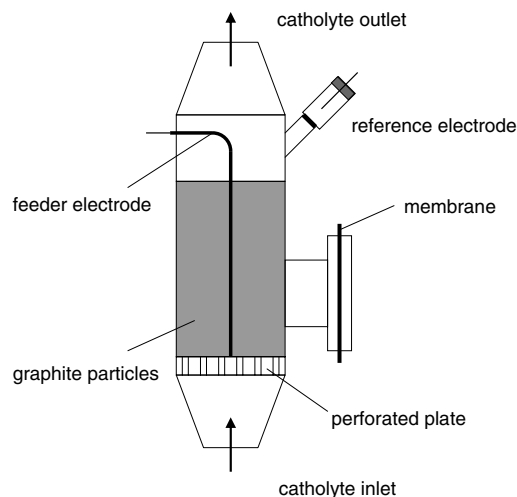


Fig. 1. Schematic of the small scale apparatus.

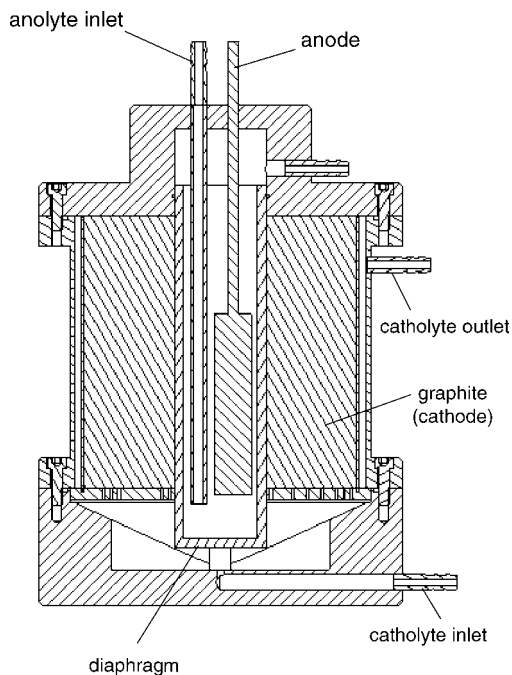


Fig. 2. Schematic of the large scale apparatus.

stainless steel grid (G. Bopp, AG, Switzerland)) and with a ceramic separator (Alsint 99,7-tube, porous,  $d = 5$  cm, FIRAG AG, Ebmatingen, Switzerland) between them. The working electrode consisted of a bed electrode made up of 2 kg of graphite granules ( $d = 2-3$  mm) with a bed depth of 5 cm and a height of 15 cm. The same electrolyte circuit was used as for the small scale reactor.

### 2.3. Electrode preparation

Four different commercial graphite granules were used after washing with distilled water three times and wetting overnight in 1 M sodium hydroxide solution: (a) enViro Gram, no. 00514, enViro Cell, Oberusel, Germany; (b) PMC, Sevierville, TN, USA, granular carbon, Lot. no. 2840; (c) TIMREX T1000-8000 graphite, Timcal group, Bodio, Switzerland; (d) Norit RX3 Extra, Lot. No. 510207, Norit Nederland BV, Amerfoort, Netherlands.

#### 2.3.1. Noble metal deposition on graphite

Platinized graphite was prepared by impregnating it with a freshly prepared hexachloroplatinic-solution, reduction with hydrazine and subsequent adsorption of the platinum particles onto the graphite [14, 15]. Graphite, as a support for palladium, was prepared by impregnating with a freshly prepared  $\text{PdCl}_2$  solution in 0.1 M sulfuric acid, reduction with hydrazine and subsequent adsorption of the palladium particles onto the graphite [15]. In addition, commercial carbon granules with 0.5 wt % platinum were used as received (PMC, Sevierville, TN, USA, 0.5%Pt/2840 granular carbon, Lot. no. 20617).

### 2.3.2. Oxidative pretreatment

The graphite was treated with concentrated and 1 M nitric acid at 25 °C and 121 °C (boiling) for 1 h. After oxidation the samples were washed with distilled water and dried overnight at 110 °C. In a second method, the graphite was soaked with a  $10^{-2}$  M solution of acidified (sulfuric acid to pH 2) potassium permanganate (1 g graphite per 10 ml of solution) for 5 h. After oxidation the samples were washed with distilled water and dried overnight at 110 °C. In a third method, the graphite was soaked with a saturated solution of sodium peroxodisulfate ( $\text{Na}_2\text{S}_2\text{O}_8$ ) in 2 M  $\text{H}_2\text{SO}_4$  (1 g graphite per 10 ml of solution) for 2 h. After oxidation the samples were washed with distilled water and dried overnight at 110 °C. Finally, in a fourth method, the graphite was kept in contact with an acidified (sulphuric acid to pH 2) 8 wt % solution of  $\text{H}_2\text{O}_2$  (1 g graphite per 10 ml of solution) in a beaker until gas evolution ceased (40 min). During this operation the temperature of the reaction mixture rose from room temperature to 45 °C. After oxidation the samples were washed with distilled water and dried overnight at 110 °C.

### 2.3.3. Modification of the graphite granules with quinones and anthraquinones

To introduce various functional groups on the graphite surface 10 g of graphite (enViro) were immersed in a 3:1 (by volume) mixture of  $\text{H}_2\text{SO}_4$ – $\text{HNO}_3$  at 100 °C for 4 h. After cooling the graphite particles were filtered off and washed with distilled water. Subsequently, the graphite was treated with 100 ml of 5% NaOH to neutralize the excess acid present followed by washing with distilled water. The granules became rather crumbly and were partly disintegrated during this procedure. Thus, too small particles were removed by sieving to guarantee a constant active surface of the electrode. The resulting oxidized graphite was dried over  $\text{CaCl}_2$  for 24 h. The carboxylic groups formed were reduced to alcoholic or phenolic functional groups by reacting 10 g graphite with 20 g of  $\text{NaBH}_4$  in 500 ml of distilled methanol. The reduction process was carried out for 12 h with constant stirring. Afterwards, methanol was removed from the slurry, and the reduced graphite washed with 500 ml of pure methanol. Benzoquinone and naphthoquinone were covalently attached to the pre-treated graphite by refluxing the pre-treated graphite and the respective quinone with  $\text{ZnCl}_2$  (1:1) in dry benzene for 78 h. The resulting material was soxhlet extracted for another 60 h using acetone as solvent. Covalent modification with anthraquinone was carried out based on a reported procedure [16, 17]. Anthraquinone carboxylic acid was first activated by stirring with *N,N'*-dicyclohexylcarbodiimide (DCC) in dry tetrahydrofuran for 24 h. The pretreated reduced graphite was added to this solution for further 24 h. The resulting material was soxhlet extracted for another 60 h using methanol as solvent.

1,2,5,8-Tetrahydroxyanthraquinone, 1-aminoanthraquinone, 2-aminoanthraquinone and 5-amino-acenaphthenequinone were immobilized by covalent modification

of the graphite via the surface carboxylic groups. The pretreated oxidized graphite was first activated by stirring with *N,N'*-dicyclohexylcarbodiimide (DCC) in dry tetrahydrofuran for 24 h. The mediator molecule was added to this solution for further 24 h. The resulting material was soxhlet extracted for another 60 h using methanol as solvent.

### 2.4. Procedure

Cathodic dispersions of indigo were usually composed of 0.1 g of indigo (sieve fraction between 0.06–0.08 mm) per litre of 1 M sodium hydroxide solution. In the large scale cell concentrations up to  $100 \text{ g l}^{-1}$  were investigated. In all experiments the solutions were deoxygenated for at least two hours before the experiment and maintained under a nitrogen atmosphere during measurements. Anodic solutions consisted of 1 M sodium hydroxide solution. Usually the reduction experiments were performed at 50 °C and a fluid flow velocity of  $1.68 \text{ cm s}^{-1}$ . In case of different pH values, the ionic strength was adjusted to 1 M NaOH (pH 14) with  $\text{Na}_2\text{SO}_4$ .

## 3. Results and discussion

From the graphite materials (enViro cell, Timcal, Norit, PMC) examined, the granular material from enViro cell proved to be the most active catalyst. Thus, this material has been used for further investigations. A series of galvanostatic runs was carried out to assess the effect of operating parameters such as current density, pH, temperature, indigo concentration and flow rate of the catholyte on the electrochemical kinetics. Laboratory dyeing experiments show a dyeing behaviour of the electrochemically reduced indigo similar to that of conventional reduction methods. In addition, in the vast majority of cases a 95% mass balance for indigo was obtained after the experiment by reoxidation to the insoluble product and filtration of the electrolyte. Therefore, it is obvious that the reaction product is stable under the applied conditions and no other products are formed.

Leuco indigo was produced – in contrast to the process based on the electrochemical reduction of the indigo radical [3–5] – directly from the indigo suspension and was identified by spectrophotometric analysis ( $\lambda_{\text{max}} = 410 \text{ nm}$ ). Thus, direct electron-transfer between indigo and the graphite seems to be the relevant process. However, it cannot be excluded that the electrochemical reduction of indigo radical occurs simultaneously to the direct reduction of the indigo pigment. Certainly, the red coloured radical species ( $\lambda_{\text{max}} = 565 \text{ nm}$ ) was formed after some time by the disproportionation of indigo with leuco indigo. Nevertheless, it is impossible that the radical-mechanism is highly significant for this process. The concentration of the radical species is very low and, consequently, so is the reduction rate.

In all experiments an induction period without formation of leuco indigo was observed between 30 and 60 min. This is due to the remaining traces of dissolved oxygen which consume a certain amount of generated leuco indigo. An increased stripping time with argon before the addition of indigo could reduce this period. However, in addition, the induction period could be reduced by the presence of indigo during the stripping time. Usually, indigo really adheres to the graphite surface, but in case of a flow-system it might also be washed away at the same time. Therefore, it takes some time until a reactive layer of indigo is formed at the graphite granules surface. If this prefiltration can take place during the stripping period, the reduction of indigo can start much earlier. Nevertheless, the production rate of leuco indigo has never been influenced by the prefiltration step.

### 3.1. Influence of current density and temperature

Reaction rate as a function of current density and temperature is shown in Figure 3. At all temperatures the reduction rate goes through a maximum with increasing current density and also increases with increasing temperature. In addition, the maxima are shifted to higher current values with increasing temperature. At 90 °C the maximum reduction rate was approximately 40 nmol min<sup>-1</sup> g<sup>-1</sup> graphite. The apparent activation energy of this electrode process was calculated from the relationship between the logarithm of the reduction rate against  $T^{-1}$  at a constant cathodic potential of -1.05 V vs Ag/AgCl 3 M and the value is  $E_A = 11.4 \pm 0.17$  kJ mol<sup>-1</sup> (95%,  $N = 4$ ). A more profound understanding can be obtained by analyzing the production rate as a function of electrode potential (Figure 4). The maximum occurs always at a potential of approximately -1200 mV vs Ag/AgCl 3 M KCl, which is close to the necessary value for the cathodic

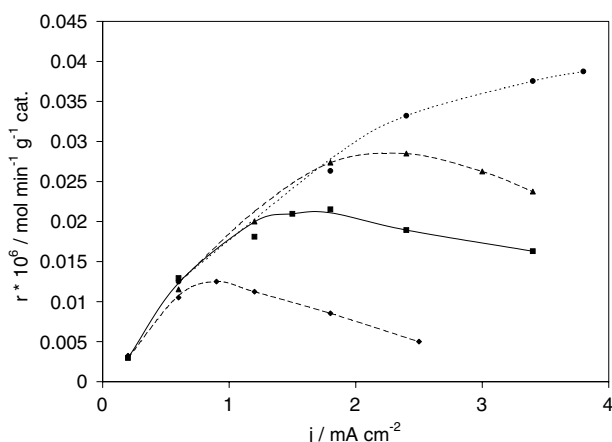


Fig. 3. Influence of current density  $j$  and temperature  $T$  on the leuco indigo production rate  $r$ . System parameters: enViro cell graphite granules, 100 mg l<sup>-1</sup> Indigo and 1 M NaOH; fluid velocity of 1.67 cm s<sup>-1</sup>. Current density is related to area of membrane (5 cm<sup>2</sup>). Key: (◆) 25, (■) 50, (▲) 75 and (●) 90 °C.

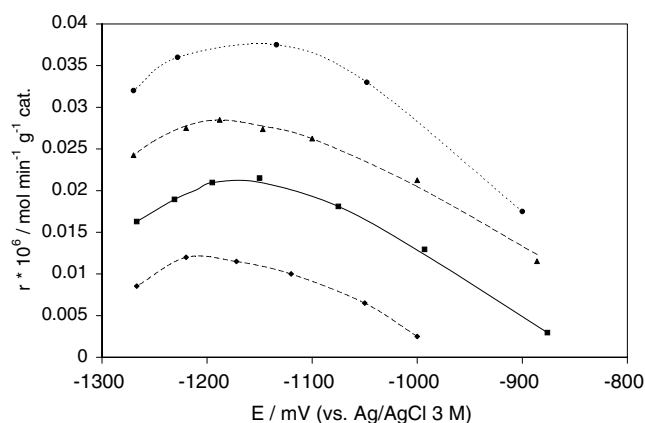


Fig. 4. Influence of cathode potential  $E$  and temperature  $T$  on the leuco indigo production rate  $r$ . System parameters: enViro cell graphite granules, 100 mg l<sup>-1</sup> Indigo and 1 M NaOH; fluid velocity 1.67 cm s<sup>-1</sup>. Current density is related to area of membrane (5 cm<sup>2</sup>). Key: (◆) 25, (■) 50, (▲) 75 and (●) 90 °C.

evolution of hydrogen. Thus, at too high values of the current density indigo is removed from the electrode surface by gas evolution and the leuco dye formation is diminished. The slight shift of the maxima to a lower potential with increasing temperature can be ascribed to the reduction in the overpotential.

Current efficiency shows a maximum of approximately 50% at a current density of 0.6 mA cm<sup>-2</sup> (Figure 5). This observation is not in agreement with theory, according to which current efficiency should increase steadily when the current density is reduced. However, at very small production rates the influence of oxygen present in the solution due to tightness problems becomes significant and may reduce the efficiency of the process.

### 3.2. Influence of pH

The effect of initial pH of the bulk solution on the efficiency of the reduction was investigated, and the

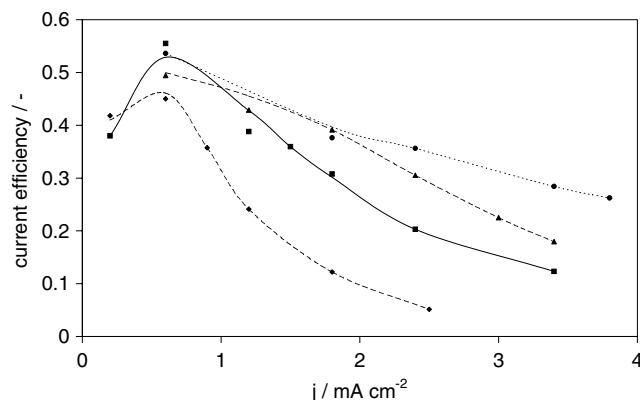


Fig. 5. Influence of current density  $j$  and temperature  $T$  on the current efficiency of the leuco indigo production rate  $r$ . System parameters: enViro cell graphite granules, 100 mg l<sup>-1</sup> Indigo, 1 M NaOH, fluid velocity of 1.67 cm s<sup>-1</sup>. Current density is related to area of membrane (5 cm<sup>2</sup>). Key: (◆) 25, (■) 50, (▲) 75 and (●) 90 °C.

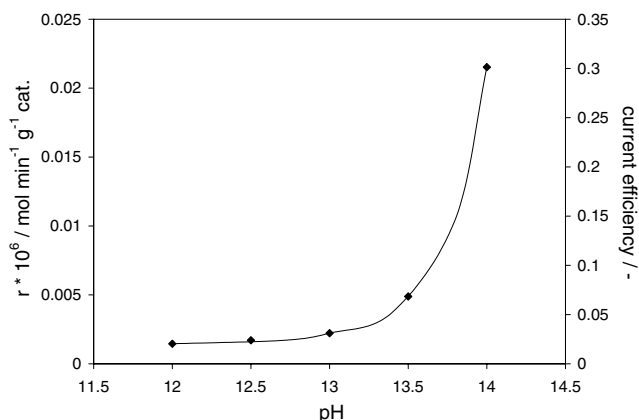


Fig. 6. Influence of pH on the leuco indigo production rate  $r$  and current efficiency. System parameters: enViro cell graphite granules,  $100 \text{ mg l}^{-1}$  Indigo. Current density ( $2 \text{ mA cm}^{-2}$ ) is related to area of membrane ( $5 \text{ cm}^2$ ),  $50 \text{ }^\circ\text{C}$  and a fluid velocity of  $1.67 \text{ cm s}^{-1}$ .

results are shown in Figure 6. The reaction rate is clearly enhanced with increasing pH. This effect might be caused by the presence of the more soluble ionic forms of leuco indigo, because non-ionic or 'acid' forms of the reduced indigo are of poor water solubility [18]. On the other hand, it is possible that on graphite the positive effect of increasing pH could be due in part to the decrease of the rate of hydrogen evolution competing with the reduction of indigo.

### 3.3. Influence of fluid velocity

The influence of fluid velocity has been analysed during batch experiments at a constant potential of  $-1200 \text{ mV}$  vs  $\text{Ag/AgCl } 3 \text{ M KCl}$  (Figure 7). A maximum in reduction rate of  $8.75 \text{ nmol min}^{-1} \text{g}^{-1}$  graphite was reached exactly at the fluidization point ( $v = 2.1 \text{ cm s}^{-1}$ ) determined by the Richardson and Zaki method [19]. Above the fluidization point the expansion of the bed causes a sharp rise in the effective resistance of the particle phase. The associated IR drop leads to a sharp

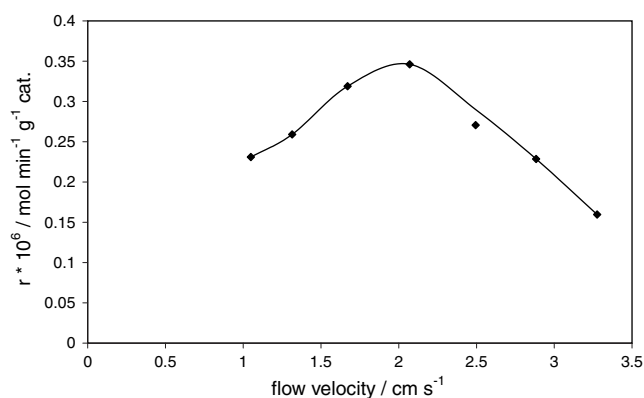


Fig. 7. Influence of fluid velocity on the leuco indigo production rate  $r$ . System parameters: enViro cell graphite granules,  $100 \text{ mg l}^{-1}$  Indigo and  $1 \text{ M NaOH}$ . Current density ( $2 \text{ mA cm}^{-2}$ ) related to area of membrane ( $5 \text{ cm}^2$ ),  $25 \text{ }^\circ\text{C}$ .

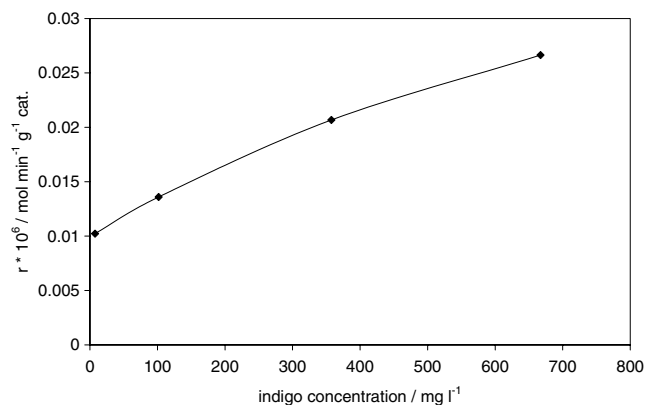


Fig. 8. Influence of indigo concentration on the leuco indigo production rate  $r$ . System parameters: enViro cell graphite granules,  $1 \text{ M NaOH}$ . Current density ( $2 \text{ mA cm}^{-2}$ ) related to area of membrane ( $5 \text{ cm}^2$ ),  $50 \text{ }^\circ\text{C}$  and fluid velocity  $1.67 \text{ cm s}^{-1}$ .

decrease in macrokinetic current density and the effective filtration layer is destroyed. Therefore, it would probably be best to use a fixed bed electrode which cannot expand (i.e., flow operation in the downward direction to press the granules against a frit) at high fluid flow rates.

### 3.4. Influence of indigo concentration

Figure 8 shows that increase in indigo concentration enhances the reaction rate. This effect is probably based on the better contact between the indigo particles and the graphite granules due to the higher probability of a collision. In addition, the adsorbed layer of indigo pigment will be stabilized by the increasing pressure drop over the fixed bed. However, a blocking of the electrode has never been observed during the experiments.

### 3.5. Influence of graphite oxidative pretreatment

Much of the chemical activity of the carbon surface is connected with quinone and hydroquinone groups, whether directly attached to the carbon black surface or part of more complex structures [20–24]. In addition, oxidative pretreatment can increase the content of oxygen-containing groups on the surface of carbon [20–30]. Therefore, it should be possible to accelerate the process by the selective generation of quinone-like functionalities on the surface of the graphite electrode.

In the first method, the graphite was treated with nitric acid under various conditions. Unfortunately, after this pretreatment no activity for indigo reduction was observed. This effect might be based on the destructive reaction of graphite with nitric acid which has been investigated by several workers [25–27]. In addition, the granules crumbled into small particles at too high concentrations of nitric acid. In the second method, the graphite was soaked with a solution of

potassium permanganate. The observed decrease in reduction rate is probably based on the decomposition of the graphite with permanganate and the formation of  $\text{MnO}_2$  on the surface of the carbon, which has been described in the literature [27–29]. In the third method, the graphite was treated with  $\text{Na}_2\text{S}_2\text{O}_8$ , but this had no influence on the reduction rate. In the fourth method, the graphite was soaked with  $\text{H}_2\text{O}_2$ . The reduction rate could be approximately doubled to a value of  $40 \text{ nmol min}^{-1} \text{ g}^{-1}$  graphite ( $50 \text{ }^\circ\text{C}$ ,  $\text{pH } 14$ ,  $2 \text{ cm s}^{-1}$ , current density  $1.5 \text{ mA cm}^{-2}$ ). Simultaneously, an increase in redox capacity could be measured by redox titration [30, 31]. Thus, the increasing catalytic activity probably correlates with the formation of quinone-like functional groups.

Surface modification of carbon electrodes by electrochemical pretreatment has been the subject of many investigations, and several reviews are available [24, 32, 33]. Thus, the influence of a preanodization step in 20%  $\text{H}_2\text{SO}_4$  at  $50 \text{ }^\circ\text{C}$  and  $0.3 \text{ A cm}^{-2}$  (related to the area of the membrane,  $5 \text{ cm}^2$ ) has also been studied. Redox capacity and reduction rate are plotted in Figure 9 as a function of charge consumed during the electrochemical oxidative pretreatment. This figure shows that both the redox capacity and the reduction rate increase steadily when the charge used to electrochemically oxidize the graphite electrode in the pretreatment procedure varies between 0 and  $200 \text{ C g}^{-1}$  graphite. An electrochemical oxidation extended and beyond a charge of  $200 \text{ C g}^{-1}$  graphite does not yield any further change. However, it is possible to accelerate the reduction rate by a factor of three to  $60 \text{ nmol min}^{-1} \text{ g}^{-1}$  ( $50 \text{ }^\circ\text{C}$ ,  $\text{pH } 14$ ,  $2 \text{ cm s}^{-1}$ , current density  $1.5 \text{ mA cm}^{-2}$ ). In addition, it was possible to activate also other graphite materials (i.e., Timrex T1000-8000 graphite, Timcal group, Bodio, Switzerland) which were inactive against indigo reduction without pretreatment. Therefore, electrochemical preanodization seems to be a very efficient technique for changing the electrochemical behaviour of graphite electrodes.

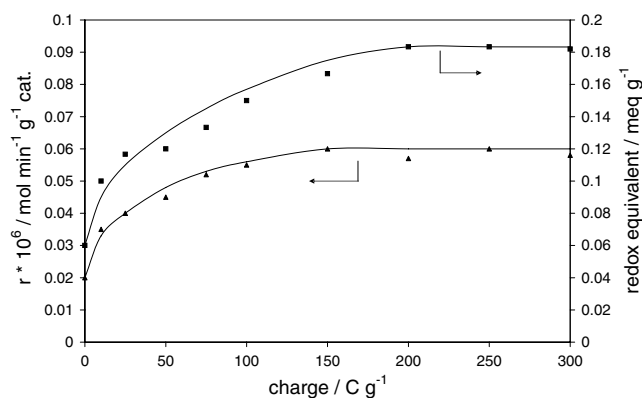


Fig. 9. Plot of leuco indigo production rate  $r$  and redox equivalent of the graphite (enViro cell graphite granules) as a function of charge consumed during electrochemical oxidation in sulfuric acid of a graphite electrode at a current density of  $50 \text{ mA cm}^{-1}$ .

### 3.6. Experiments with quinone modified graphite granules

Another interesting approach to enhance the electrocatalytic properties of the graphite material is based on the covalent bonding of quinoid molecules onto the graphite surface [16, 34]. Thus, electron transfer mediators which can undergo fast electron transfer with the electrode and also with the substrate (indigo) are immobilized on the carbon electrode. In the particular case of indigo reduction quinones and anthraquinones has been used as redox-active molecules. These substances are already well known from the mediator process [35]. In addition, such species have been used as catalysts for the chemical vatting process [36].

Covalent modification of graphite was carried out according to a reported procedure [16, 34]. However, it is well known that quinones strongly physisorb onto graphite particles and even after 60 h of Soxhlet extraction, some physisorbed molecules were observed to be present [16, 37]. Thus, it cannot be excluded that there is a certain amount of physisorbed species present after the modification procedure.

The catalytic activity of the quinone and anthraquinone modified electrodes were demonstrated by carrying out preliminary studies on the reduction of indigo. The catalytic activity of the electrodes depends both on the amount or surface concentration and the nature of the attached species. Thus, the reduction rate has been normalized by the redox capacity of the graphite, which correlates with the amount of quinone-like functional groups (Table 1). 5-Amino-acenaphtheneanthraquinone and 1,8-dihydroxyanthraquinone are among the most active catalysts and it is possible to increase the normalized reduction rate in comparison to the unmodified reference material. All other immobilized species show lower activity than the reference graphite. In addition, it is somewhat surprising that 1-aminoanthraquinone is much more active than its isomer 2-aminoanthraquinone. Usually the redox reactions take place at similar potentials [38]. Probably the two isomers align itself in different orientations to the graphite surface. Thus, different electronic interactions have a bearing on the redox activity [38].

Table 1. Influence of several immobilized quinone and anthraquinone molecules on the indigo reduction rate  $r$  ( $40 \text{ g}$  graphite (enViro),  $50 \text{ }^\circ\text{C}$ ,  $\text{pH } 14$ ,  $2 \text{ cm s}^{-1}$ , current density  $1.5 \text{ mA cm}^{-2}$ )

Immobilized mediator	Reduction rate $r$ / $\text{nmol min}^{-1} \text{ meq}^{-1}$
enViro cell graphite (reference)	347
Benzoquinone	25
Naphthoquinone	58
1-Aminoanthraquinone	231
2-Aminoanthraquinone	150
Anthraquinone-2-carboxylic acid	245
5-Aminoacenaphtheneanthraquinone	450
1,8-Dihydroxyanthraquinone	389

However, it is important to mention, that all modified electrodes showed a lower reduction rate per gram material than the reference material. Therefore, the surface concentration of the immobilized molecules should be increased by more efficient techniques. Preliminary experiments with acid chloride groups instead of the surface carboxylic groups or dichlorotriazine or  $\beta$ -sulphato-ethylsulphonyl reactive groups as anchor molecules reacting with amino or hydroxyl groups at the graphite surface indicated a significant higher catalytic activity of the electrode [31].

### 3.7. Experiments with noble metals supported on the graphite

On graphite no chemisorption or only very weak chemisorption of hydrogen is possible. Thus, normal electron transfer seems to be the relevant process for the reduction of indigo. On the basis of recently presented experiments on the electrocatalytic hydrogenation (ECH) of indigo [8–9], it should be possible to improve the process by immobilizing noble metal particles on the graphite granules surface. Therefore, three different types of catalyst were investigated: on one hand commercial crushed coconut shell based carbon granules with 0.5 wt % Pt (PMC, Sevierville, TN, USA) and on the other hand electrographite granules (enViro Cell, Oberusel, Germany) as support for platinum and palladium. The latter material, especially with Pd as catalyst, showed a much higher activity against indigo reduction (Table 2). However, the coconut shell based carbon granules without Pt have, in contrast to the electrographite, no activity against the reduction of indigo. Therefore, the reduction activity can be correlated to the hydrogenation process induced by the platinum content. In addition, the nature of the noble metal dispersed onto the carbon has a determining effect on the efficiency of the reduction process based on ECH. This might be due to the competition between the hydrogen evolution and the hydrogenation process. In the Pt/C system, the rate of hydrogen desorption, respectively the Heyrovský and Tafel steps of the hydrogen evolution, is much faster than that for hydrogenolysis, which results in a poor efficiency of ECH. On the other hand, for the Pd/C catalyst, hydrogenolysis and hydrogen desorption have comparable rates, resulting in fair and good electrogenolysis efficiencies.

Table 2. Influence of different noble metals on graphite as supporting material on the leuco indigo production rate  $r$

Electrode material	Reduction rate $r$ / $\mu\text{mol min}^{-1} \text{meq}^{-1}$
enViro cell graphite (reference)	0.024
enViro cell graphite + 0.5 wt % Pt	0.032
enViro cell graphite + 0.5 wt % Pd	0.049
PMC carbon + 0.5 wt % Pt	0.010

### 3.8. Results and discussion in the large-scale cell

According to the results achieved with the small-scale reactor, preliminary experiments were performed with preanodized enViro cell graphite ( $200 \text{ C}^{-1} \text{g}^{-1}$ ,  $50 \text{ }^\circ\text{C}$ , pH 14,  $2 \text{ cm s}^{-1}$ , current density  $50 \text{ mA cm}^{-2}$ ) at pH 14, with a fluid flow of  $2 \text{ cm s}^{-1}$ , a diaphragm current density of  $1 \text{ mA cm}^{-2}$  ( $240 \text{ cm}^2$ ),  $10 \text{ g l}^{-1}$  indigo and  $50 \text{ }^\circ\text{C}$ . In these conditions, the following results were obtained:

Current efficiency 61%

Specific productivity  $10 \text{ mg min}^{-1} \text{kg}^{-1}$  graphite

Mean voltage 2.8 V

Power consumption  $1 \text{ kWh kg}^{-1}$

Although the scale of the reactor was increased by a factor of 30, and experiments were performed at an indigo concentration up to  $10 \text{ g l}^{-1}$ , it was still possible to reduce indigo without blocking of the reactor. Moreover, current efficiency and reduction rate were slightly enhanced. Thus, to achieve the common industrial leuco indigo production rates of  $200 \text{ g min}^{-1}$ , a reactor size of approximately  $20 \text{ m}^3$  graphite would be necessary. However, this discovery seems to be of future interest, both from an economical and ecological point of view, for the industrial application of an electrochemical vatting process.

## 4. Conclusions

Graphite granules were used as electrode material in a fixed- and fluidized bed reactor to address the question of the industrial feasibility of this new direct electrochemical reduction method for vat dyes. Optimized conditions in the system were sought, and a scale-up in indigo concentration to  $10 \text{ g l}^{-1}$  was achieved. Increasing pH and temperature can enhance the reduction rate, and a maximum conversion has been found by optimizing current density and flow velocity in the reactor. Special pretreatment of the graphite (i.e., soaking with hydrogen peroxide or preanodization) enhances the reduction rate by inducing the formation of quinone-like functional groups. Immobilizing noble metal particles on the graphite surface cause electrocatalytic hydrogenation in addition to the electron transfer process resulting in fair and good electrogenolysis efficiencies.

These results are a basis for the further development of a cheap, continuously and ecologically working cell for the direct electrochemical reduction of dispersed indigo and other vat dyes. Especially, the introduction of surface functionalities by chemical reaction routes is at present an exciting research area. Hopefully, the immobilization of redox-active substances (i.e., metal complexes) will lead to even higher reduction rates. However, the next step will be pilot-plant trials after a scale-up procedure. Increasing the reactor size and indigo concentration to more than  $100 \text{ g l}^{-1}$  may cause a blocking of the fixed bed. Therefore, optimization of the cell design will be a requirement for the successful realization of this method.

## Acknowledgements

The authors would like to acknowledge the companies 'Tex-A-Tec AG', Wattwil, Switzerland (W. Marte), ElectroCell AB, Täby, Sweden (J. and P. Bersier, L. Carlsson), enViro Cell, Oberursel, Germany (K. Müller, W. Dietz), Timcal, Bodio, Switzerland (M. Spahr) and Activated Metals & Chemicals/PMC, Sevierville, TN, USA (S. Doughty) for valuable support and discussion. Peter Wägli, Laboratory of Solid State Physics, ETH Zurich, is acknowledged for SEM studies and Philippe Trüssel, LTC workshop, ETH Zurich for the excellent construction of the reactor and the flow circuit. ETH Zurich, Commission for Technology and Innovation (CTI) as well as the Hartmann-Müller-Fonds is acknowledged for financial support.

## References

1. W. Marte, *Int. Text. Bull., ITB Veredlung* **41** (1995) 33.
2. T. Bechtold and A. Turcanu, *J. Electrochem. Soc.* **149** (2002) D7.
3. A. Roessler, O. Dossenbach, U. Meyer, W. Marte and P. Rys, *Chimia* **55** (2001) 879.
4. A. Roessler, D. Crettenand, O. Dossenbach, U. Meyer, W. Marte and P. Rys, *Electrochim. Acta* **47** (2002) 1989.
5. A. Roessler, O. Dossenbach, W. Marte and P. Rys, *J. Appl. Electrochem.* **32** (2002) 647.
6. C. Merk, J. Botzem, G. Huber and N. Grund, *Patent WO 01/46497* (2001).
7. C. Merk, G. Huber and A. Weiper-Idelmann, in J. Yoshida, D.G. Peters, M.S. Workentin, (Eds), *Reactive Intermediates in Organic and Biological Electrochemistry*, In Honor of the Late Professor Eberhard Steckhan, **PV 2001-14** (The Electrochemical Society Proceedings Series, Washington, DC, 2001), p. 121.
8. A. Roessler, O. Dossenbach and P. Rys, *J. Electrochem. Soc.* **150** (2003) D1.
9. A. Roessler, O. Dossenbach, W. Marte and P. Rys, *Dyes and Pigment* **54** (2002) 141.
10. A.M. Bond, F. Marken, E. Hill, R.G. Compton and H. Hügel, *J. Chem. Soc., Perkin Trans. 2* **28** (1997) 1735.
11. S. Komorsky-Lovric, *J. Electroanal. Chem.* **482** (2000) 222.
12. M. Rowe and J.St.H. Davies, *J. Chem. Soc.* **117** (1920) 1344.
13. M. Lauwiner, P. Rys and J. Wissmann, *Applied Catalysis, A: General* **172** (1998) 141.
14. F. Atamny and A. Baiker, *Surf. Interface Anal.* **27** (1999) 512.
15. H. Bönemann, W. Brijoux, R. Brinkmann, E. Dinjus, T. Jousen and B. Korall, *Angew. Chem.* **103** (1991) 1344.
16. P. Ramesh and S. Sampath, *Analyst* **136** (2001) 1872.
17. J.C. Sheehan and G.P. Hess, *J. Am. Chem. Soc.* **77** (1955) 1067.
18. J.N. Ethers, *J. Soc. Dyers Colourists* **109** (1993) 251.
19. J.F. Richardson and W.N. Zaki, *Trans. Inst. Chem. Eng.* **32** (1954) 35.
20. Y.G. Ryu, S.I. Pyun, C.S. Kim and D.R. Shin, *Carbon* **36** (1998) 293.
21. B. Donnet, *Carbon* **6** (1968) 161.
22. V.A. Garten and D.E. Weiss, *Aust. J. Chem.* **10** (1957) 309.
23. V.A. Garten and D.E. Weiss, *Aust. J. Chem.* **8** (1955) 68.
24. K. Kinoshita, 'Carbon, Electrochemical and Physicochemical Properties' (J. Wiley & Sons, New York, 1998).
25. N.N. Nemerovets, V.F. Surovikin, S.V. Orekhov, G.V. Sazhin and N.G. Saovnichuk, *Solid Fuel Chemistry (Engl. Transl. of Khim. Tverd. Topl.)* **14** (1980) 104.
26. L.P. Gilyazetdinov, V.I. Romanova, A.S. Lutokhina, É.I. Tsygankova and I.M. Safronova, *J. Appl. Chem. USSR (Engl. Transl. of Zhurnal Prikladnoi Khimii)* **49** (1976) 420.
27. M. Acedo-Ramos, V. Gomez-Serrano, C. Valenzuela-Calahorra and A.J. Lopez-Peinado, *Spectrosc. Lett.* **26** (1993) 1117.
28. A.V. Melezhik, L.V. Makarova and A.A. Chuiko, *Russian J. Inorg. Chem. (Engl. Transl. Zhurnal Neorganicheskoi Khimii)* **34** (1989) 196.
29. A. Banerjee, B.K. Mazumdar and A. Lahiri, *Nature* **193** (1962) 267.
30. A. Voet and A.C. Teter, *Am. Ink Maker* **38** (1960) 44.
31. A. Roessler, PhD thesis No. 15 120, ETH Zurich (2003).
32. R.L. McCreery, *Electroanal. Chem.* **17** (1991) 221.
33. R.C. Engstrom, *Anal. Chem.* **54** (1982) 2310.
34. J. Schreurs and E. Barendrecht, *Recl. Trav. Chim. Pays-Bas.* **103** (1984) 205.
35. T. Bechtold, E. Burtscher and A. Turcanu, *J. Electroanal. Chem.* **465** (1999) 80.
36. K.S. Tschyong and F.I. Sadow, *Textil Praxis* **24** (1969) 454.
37. A.P. Brown and F.C. Anson, *Anal. Chem.* **49** (1977) 2589.
38. M. Sharp, *Electrochim. Acta* **23** (1978) 287.